(12) INTERNATIONAL APPLICATION PUBLISHED UNDER THE PATENT COOPERATION TREATY (PCT)

(19) World Intellectual Property Organization
International Bureau

(43) International Publication Date
08 April 2021 (08.04.2021)

WIPO | PCT

(10) International Publication Number
WO 2021/064446 A1

(51) International Patent Classification:
A61N 1/16 (2006.01)

(21) International Application Number:
PCT/IB2019/058334

(22) International Filing Date:
01 October 2019 (01.10.2019)

(25) Filing Language: English

(26) Publication Language: English

(72) Inventor; and
(71) Applicant: **SEROV, Igor** [RU/ES]; Avda Santa Clotilde 22 24 P03 1 B, Girona (ES).

(74) Agent: **KLIMAITIENE, Otilija**; A. Gostauto 40B, LT-03163 Vilnius (LT).

(81) **Designated States** *(unless otherwise indicated, for every kind of national protection available)*: AE, AG, AL, AM, AO, AT, AU, AZ, BA, BB, BG, BH, BN, BR, BW, BY, BZ, CA, CH, CL, CN, CO, CR, CU, CZ, DE, DJ, DK, DM, DO, DZ, EC, EE, EG, ES, FI, GB, GD, GE, GH, GM, GT, HN, HR, HU, ID, IL, IN, IR, IS, JO, JP, KE, KG, KH, KN, KP, KR, KW, KZ, LA, LC, LK, LR, LS, LU, LY, MA, MD, ME, MG, MK, MN, MW, MX, MY, MZ, NA, NG, NI, NO, NZ, OM, PA, PE, PG, PH, PL, PT, QA, RO, RS, RU, RW, SA, SC, SD, SE, SG, SK, SL, SM, ST, SV, SY, TH, TJ, TM, TN, TR, TT, TZ, UA, UG, US, UZ, VC, VN, ZA, ZM, ZW.

(84) **Designated States** *(unless otherwise indicated, for every kind of regional protection available)*: ARIPO (BW, GH, GM, KE, LR, LS, MW, MZ, NA, RW, SD, SL, ST, SZ, TZ, UG, ZM, ZW), Eurasian (AM, AZ, BY, KG, KZ, RU, TJ, TM), European (AL, AT, BE, BG, CH, CY, CZ, DE, DK, EE, ES, FI, FR, GB, GR, HR, HU, IE, IS, IT, LT, LU, LV, MC, MK, MT, NL, NO, PL, PT, RO, RS, SE, SI, SK, SM, TR), OAPI (BF, BJ, CF, CG, CI, CM, GA, GN, GQ, GW, KM, ML, MR, NE, SN, TD, TG).

Declarations under Rule 4.17:
— *of inventorship (Rule 4.17(iv))*

Published:
— *with international search report (Art. 21(3))*
— *with amended claims and statement (Art. 19(1))*

(54) **Title:** METHOD FOR PROTECTING BIOLOGICAL OBJECTS FROM THE NEGATIVE INFLUENCE OF TECHNOGENIC ELECTROMAGNETIC RADIATION

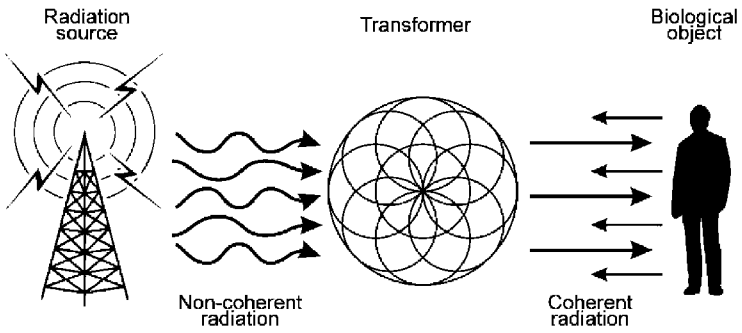

FIG. 1

(57) **Abstract:** The method for protecting biological objects (BO) from the negative influence of technogenic electromagnetic (EM) radiation in a wide range of frequencies, which consists of creating a coherent field in the form of a fractal matrix around a biological object using a fractal-matrix as coherent transducer based on a self-affine annular raster lattice (resonator) formed from ringed topological lines, which create a slit-like raster, and is a universal Fourier transformer that harmonizes the amplitude, phase, frequency and polarization vector of external technogenic radiation and the BO's own EM radiation. The transformation of external radiation occurs in accordance with the Fourier transform with the formation of a coherent matrix of EM wave superpositions. The coherent matrix does not conflict with the BO. The transformation does not affect the functioning of the technical devices. The coherent transformer can be placed on the BO, or between the BO and the source.

WO 2021/064446 A1

METHOD FOR PROTECTING BIOLOGICAL OBJECTS FROM THE NEGATIVE INFLUENCE OF TECHNOGENIC ELECTROMAGNETIC RADIATION

FIELD OF INVENTION

The invention relates to methods for protecting biological objects from the negative influence of technogenic electromagnetic radiation in a wide range of frequencies. The invention relates to protective technologies, industrial and sanitary hygiene, and occupational safety.

BACKGROUND ART

The invention relates to methods for protecting biological objects (BO) from technogenic electromagnetic (EM) radiation in a wide range of frequencies and can be used in the everyday life of each person to protect against the negative influence of surrounding technogenic radiation, including 5G mobile communication systems (3.5-28 GHz).

Known methods for protecting, blocking, scattering and absorbing a signal: RU2194376, RU2265898, RU2234175.

Patent RU2194376 / WO1997034459 relates to a method of transferring a layer onto a detail which shields against electromagnetic radiation. The layer is transferred with a predetermined extension directly or indirectly on to the detail with the help of a known printing method.

Patent RU2265898 relates to protection from electromagnetic emission. It describes mesh of electric-conductive material which is positioned on dielectric transparent film with applied transparent electric-conductive layer, made either of indium, or of tin, or of indium/tin alloy with thickness, approximately equal to 0.1 of skin layer, and the very mesh is applied with thickness not exceeding skin-layer by printer or plotter using electric-conductive compound, consisting of ultra-dispersive electric-conductive powder with stable electric conductivity and average size of particles 10.0-600.0 nm, polymer linking component, organic solvent and surfactant with certain ratio of components. The obtained effect is forming of

transparent screens, screening properties of which do not depend on falling angle of electromagnetic emission, also light and simple to manufacture.

Patent DE10039125A1 / RU2234175 discloses electromagnetic absorber granulate consisting of a highly porous glass and/or ceramic granulate coated or filled with ferrite and/or an electrically conducting material. An independent claim is also included for a process for the production of a coated absorber granulate comprising finely grinding the ferrite and/or electrically conducting material, and applying with a binder as suspension to the glass and/or ceramic granulate. Preferred Features: The electrically conducting material is a metal and/or carbon. The granulate grain size is 0.2-5 mm and the coating has a thickness of 10-300 mu m. The ferrite is made of an Mn-Zn, Ni-Zn, Ba, Sr ferrite or a Sc-, Co-, or Ti-substituted hexaferrite with a garnet structure.

The shortcoming of these methods is the loss of the signal, its distortion, a change of the natural background, inconvenience, and complexity of use.

Before proceeding to the description of the invention, it should be noted that all methods for protecting a biological object from technogenic EM radiation come down to reducing the intensity of the EM pulse, reducing the exposure time, or increasing the distance from the biological object to the radiation source, which leads to inconvenience or the inability to properly use the source of EM radiation, especially when using it to transmit large amounts of information.

SUMMARY OF INVENTION

The task for which the claimed invention is intended is to protect a biological object, in particular the human body, from the negative influence of technogenic EM radiation of a wide range of frequencies without reducing the effectiveness of the sources generating it and without imposing additional requiremlents on them.

In this aspect, it is most rational to change the structure of the EM pulse arising from the radiation source, transforming it into a form safe for the BO, without losing its effectiveness.

The restructuring of technogenic EM radiation in the proposed method implies changing its amplitude-frequency spectrum from an arbitrary form to a coherent form through the influence of a coherent field created by a transformer

that initiates the process of counter-harmonization of amplitudes, phases, frequencies, polarization vectors, and the EM radiation incident on it.

This process, which is implemented by using a coherent transformer (resonator), is proven and protected (Russian Federation Patent No. 2231137, No. 2217181, No. 2284062) and is later described in more detail.

The coherent transformer can be placed on the biological object BO, next to it, on the source of technogenic radiation, or between the BO and the source (**FIG. 1**).

DESCRIPTION OF DRAWINGS

In order to understand the invention better and appreciate its practical applications, the following pictures are provided and referenced. Figures are given as examples only and in no way shall limit the scope of the invention.

FIG. 1 depicts that the coherent transformer placed on the biological object next to it, on the source of technogenic radiation, or between the biological object and the source.

FIG. 2 presents an image of a self-affine lattice fixed on a solid medium (FIG. 2a), and a photograph of the holographic response resulting from the incoherent EM radiation's interaction with the slit topological surface of the lattice (FIG. 2b).

FIG. 3 depicts a wafer of silicon carbide (SiC), which is a source of coherent, nearly monochrome radiation at a distance of 100 nm from the surface of the wafer.

FIG. 4 depicts affine transformations of a vector.

FIG. 5 is the result of performing affine transformations.

FIG. 6 depicts appearance of a self-affine structure.

FIG. 7 modeling result for incident radiation with a frequency of 2 periods per 1 rotation by the angle φ; FIG 7a – amplitude; FIG 7b – phase.

FIG. 8 is presented periodic behavior of incident radiation of 64 periods per 1 rotation by angle φ. FIG 8a – amplitude; FIG 8b – phase.

FIG. 9 is presented distribution of strength E across the wafer's surface under the steady state; various projections.

FIG. 10 is presented distribution of the amplitude's spectral power density on the wafer's surface through time $t>t_{est}$. FIG 10a – amplitude; FIG 10b – phase.

FIG. 11 is presented result of the experiment while illuminating the surface of the resonator's wafer by a halogen lamp.

FIG. 12 is presented the resonator's surface lying in plane *x0y* with the origin at the center of the resonator. The *z*-axis is orthogonal to this plane.

FIG. 13 presents influence on 3 points with an ungrounded center.

FIG. 14 is presented electric field strength above the resonator. Development of a spatial wave from the surface of the resonator (lower graph), side view.

FIG. 15 is the strength distribution over height, to a height of 0.03 mm, with influence on 3 points with an ungrounded center.

FIG. 16 is impulse effect on two opposite points with ungrounded resonator center.

FIG. 17 is electric field strength above the resonator. Development of a spatial wave from the surface of the resonator (lower graph), side view.

FIG. 18 is electric field strength on the surface of the resonator (lower graph, $z=0$) and so on in layers above the surface: 0.1mm; 0.2mm; 0.3mm.

FIG. 19 is electric field strength for the steady state, when using a resonator with a double-sided design, side view.

FIG. 20 is electric field strength: (a) on the resonator's surface; (b) at a distance of 0.1 mm above the surface of the resonator; (c) at a distance of 0.2 mm; (d) at a distance of 0.3 mm; (e) at a distance of 0.4 mm; (f) at a distance of 0.5 mm; (g) at a distance of 0.6 mm; (h) at a distance of 0.7 mm; (i) at a distance of 0.8 mm; (k) at a distance of 0.9 mm; (l) at a distance of 1 mm; (m) at a distance of 1.1 mm; (n) of at a distance 1.2 mm; (o) at a distance of 1.3 mm; (p) at a distance of 1.4 mm; (r) at a distance of 1.5 mm; (s) at a distance of 1.6 mm; (t) at a distance of 1.7 mm.

FIG. 21 presents dynamics of changes in the strength of the field above the wafer.

FIG. 22 presents distribution of field strength E above the resonator from 0.28 to 14.18 (V/m) with incident radiation at 2.4 GHz;

FIG. 23 presents distribution of field intensity I above the resonator from 0.08 to 201.05 (W/m^2) with incident radiation at 2.4 GHz.

FIG. 24 presents simplified versions of planar projections of the spatial structural-holographic self-affine matrix of the resonator's coherently transforming field response.

DETAILED DESCRIPTION OF PREFERRED EMBODIMENTS

The claimed method is based on self-affine holographic objects' ability to transform the EM pulses interacting with them according to their characteristics.

Holography (from ancient Greek: ὅλος - whole, γράφω - I writing) is based on two physical phenomena — diffraction and interference of EM waves. The physical idea is that under the imposition of several wave pulses, under certain conditions, an interference pattern occurs, that is, a spatial regular system of maxima and minima of the intensity of electromagnetic radiation in the form of a stationary field having a fractal self-affine structure.

According to contemporary scientific concepts, when interacting with external EM radiation, any regular structure creates a periodic EM field (superposition).

In order for this interference pattern to be stable for the time necessary to observe, and in order for it to be recorded, these EM pulses must be harmonized spatially and temporally across frequencies and amplitudes. Such EM waves are called coherent.

Based on the principle of superposition, if EM waves coincide in phase, then they add with each other and produce a resultant wave with an amplitude equal to the sum of their amplitudes. If they meet in antiphase, then they cancel each other out. If two opposite EM pulses are identical in phase, amplitude, frequency, and polarization vectors, then their amplitudes are multiplied.

The resulting interaction of two coherent waves is a fractal standing wave. That is, the interference pattern will be stable in time (phase), in amplitude (power), polarization vector (direction), and frequency (stability). Since any fractal

construct is a self-affine structure, that is, formed from its own analogues, this property underlies the production and restoration of holograms in its individual fragments.

To obtain a holographic response, the resonator must either itself have the ability to transform the radiation incident on it into a coherent form, or the incident radiation must initially be coherent. The hologram arising from the resonator carries not only the same characteristics and properties as the radiation incident on the resonator, but also the specific features of the resonator topology itself. As a result, if the resonator initiates a coherent transformation of incoherent EM radiation incident on it, the resulting hologram has the same ability to transform an EM pulse of the corresponding frequency range that interacts with it into a coherent state.

The strength and intensity of the coherent field fall in proportion to the square of the distance from the resonator. Thus, the given EM field can transform EM radiation interacting with it into a coherent form, if its strength and intensity is not lower than the strength and intensity of the opposite radiation. Such interaction is possible due to the fractality of the resonator, not only when the frequencies coincide, but also when they are similar at multiple scales.

FIG. 2 presents an image of a self-affine lattice fixed on a solid medium (**FIG. 2a**), and a photograph of the holographic response resulting from the incoherent EM radiation's interaction with the slit topological surface of the lattice (**FIG. 2b**).

It is known that coherence (cohaerens - in communication) is the harmonized flow in time and in space of several oscillatory processes.

The term "coherence" means the absence of conflicts, consistency, and communication. When applied to EM radiation, it refers to consistency and communication between EM oscillations and waves. Because radiation is distributed across time and space, it is possible to estimate the coherence of oscillations radiated by a source at various points in time at any particular point in space, as well as the coherence of oscillations radiated at a particular point in time at various points in space [8]. Oscillations are called fully coherent if the difference of their phases at the observation point remains constant in time and, when these oscillations are added, determines the amplitude and intensity of the summed

(resulting) oscillation. Oscillations (waves) are called partially coherent if the difference of their phases changes very slowly (compared with the observation time), and incoherent if the phase difference changes randomly.

Thus, "coherence" means consistency and communication between EM oscillations. EM radiation is distributed across time and space, so it is possible to estimate the coherence of oscillations radiated by a source at various points in time at any particular point in space (temporal coherence) or the coherence of oscillations radiated at a particular point in time at various points in space (spatial coherence). These properties lead to the conclusion that energy losses at a point of coherent radiation are minimized.

An example of obtaining coherent radiation using a novel approach is creating regular structures on the surface of solids. These structures then act as resonators. An example of this approach [9] is the use of a SiC wafer with a regular structure in the form of parallel grooves, which initiates the production of coherent radiation with a peak at the corresponding wavelength **(FIG. 3)**.

Of interest is the case where it would be possible to generate EM oscillations on not a single frequency, but a wide range of frequencies, while preserving interrelationships between them such that they remain coherent, not only in time, but also in space, like a laser. To do this, we need to use, as a foundation, a certain resonator on a planar substrate, similar to the given example, but with a topographical surface in the form of fractally arranged circles with specific interrelationships.

A device that generates coherent radiation with such properties would find application in a diversity of fields, including for spatial encoding of data, because it can transform incident radiation into a coherent form with properties containing information about the incident radiation.

So-called self-affine structures generated in the form of annular slits open unexpected possibilities for use in scientific research and technology. In [1] a self-affine fractal is defined as a structure that is invariant after simultaneous yet quantitatively different changes in the scale along different spatial axes. The affine transformation of a vector from the origin to point (x_1, y_1), to a vector from point (b_1, b_2) to point (x_2, y_2) is defined as:

$$x_2 = a_{11}x_1 + a_{12}y_1 + b_1$$
$$y_2 = a_{21}x_1 + a_{22}y_1 + b_2$$

System (1) can be represented as a matrix:

$$T = \begin{bmatrix} a_{11} a_{12} b_1 \\ a_{21} a_{22} b_2 \end{bmatrix}$$

and illustrated in **FIG. 4.**

Affine transformations can also define a rotation by angle *a* about the origin.

After performing transformations representing the multiplication of points of the figure by the scale factor $m_1 = 2^i$ and rotations by an angle proportional to the coefficient $m_2 = 2^j$, and overlaying the original drawing, we obtain the figure shown in **FIG. 5.**

The appearance of such a structure is presented in **FIG. 6**.

Modeling. During the modeling, a stationary model and two-dimensional and three-dimensional non-stationary models were analyzed.

Stationary model. For the stationary case, the interaction of EM radiation waves with the wafer's surface can be written as follows:

$$\frac{\partial^2 \mathbf{E}}{\partial \varphi^2} + \frac{\partial^2 \mathbf{E}}{\partial r^2} = \left(k^2 - \varepsilon \left(\frac{\omega}{c} \right)^2 \right) \mathbf{E}$$

where *k* is the wave number, *ε* is the wafer's dielectric constant, *ω* is the cyclic frequency, *c* is the speed of light; *r* is the length of the radius vector, *φ* is the polar angle, **E** is the electric component of the strength vector.

The following type of model was used during modeling:

$$\frac{\partial^2 E}{\partial \varphi^2} + \frac{\partial^2 E}{\partial r^2} = -a^2 E - b$$

where *E* is a function proportional to the strength of the radiation; *r* is the length of the radius vector, *φ* is a polar angle, *a* and *b* are constants.

During calculations on a computer, the radiation's periodic behavior was changed relative to the size of the wafer, when the wavelength of the incident radiation and the periodic behavior of the resonator's surface pattern were compared, taking into account its dimensions.

The obtained modeling results, shown in the figures **FIG. 7** and **FIG. 8**, show that the strength of the electric field, after interacting with the self-affine fractal lattice, is redistributed so that the graphs of the field distribution over the surface become regular, a trait that remains almost unchanged when changing the frequency of the incident radiation over a wide range.

Non-stationary model. The fractal served as the foundation for building the mathematical model.

The rings on the surface are grooves about 1.3 microns deep and 1 μm wide. The minimum distance between the "grooves" is 1 μm. The wafer's outer diameter was 6 mm. When interacting with the conductor, an electric field causes charges to shift and increases the concentration of charges in the "grooves" relative to adjacent areas.

Therefore, during modeling, it was assumed that the medium's charges would be concentrated more in the "grooves" than in other areas. When the potential reaches some critical value, there is a discharge along the shortest distance between the grooves.

Non-stationary two-dimensional model. In this case, the mathematical model looks like this:

$$\frac{\partial E}{\partial t} = D(\frac{\partial^2 E}{\partial x^2} + \frac{\partial^2 E}{\partial y^2}) - aE$$

where *D* and *a* are coefficients, *E* is the electric field's strength, *x* and *y* are coordinates, *and t* is time. The discharge criteria is implemented as follows: if $|E| > E_{кр}$, then $E = 0$.

The main result of the modeling is that regardless of the conditions at the boundary, the steady-state solution is stable and soliton-like. Its shape does not change with changing boundary conditions. This means that the resonator's self-affine surface transforms radiation in such a way that the result of this process does not depend on the characteristics of the radiation incident on it.

The results of the calculations for the two-dimensional model (5) are given in the figures **FIG. 9** and **FIG. 10**. **FIG. 9** shows distribution of strength *E* across the wafer's surface under the steady state; various projections. **FIG. 10** shows

distribution of the amplitude's spectral power density on the wafer's surface through time $t>t_{est}$. Amplitude is presented in **FIG. 10a**, phase – in **FIG. 10b**.

For comparison, the result of the experiment while illuminating the wafer's surface (illuminating the surface of the resonator's wafer by a halogen lamp) is presented in **FIG. 11**. The figure clearly shows a luminous "scaly" dome (hologram), similar to the results of a computational experiment.

Non-stationary three-dimensional model. A three-dimensional model was considered:

$$\frac{\partial E}{\partial t} = D(\frac{\partial^2 E}{\partial x^2} + \frac{\partial^2 E}{\partial y^2} + \frac{\partial^2 E}{\partial z^2}) - aE$$

Technically, this model only differs from the two-dimensional model by the presence of a third spatial coordinate *z*. However, this makes it possible to create a more complete representation of the interaction of the self-affine topological surface with radiation, and obtain the spatial distribution of strength *E*. The resonator's surface lies in plane *x0y* with the origin at the center of the resonator and the *z*-axis is orthogonal to this plane (**FIG. 12**).

Impulse effect on three opposite points with an ungrounded resonator center. Result of modeling with an impulse effect on three points positioned at an angle of 120° from each other (**FIG. 13**).

The graphs of the distribution of the electric field strength above the resonator in the figure **FIG. 14**. Development of a spatial wave from the surface of the resonator (lower graph) is provided by the side view. The graphs were made for heights *z* above the surface of the resonator, from *z*=0, lower graph, to *z*=0.02 mm for the last, upper graph. The wave attenuates after a height of 0.02 mm.

The figure **FIG. 15** also illustrates the strength distribution over height, to a height of 0.03 mm, with influence on 3 points with an ungrounded center.

Impulse effect on two opposite points with ungrounded resonator center. The field acts on diametrically opposite points on the surface of the resonator, which lie in the middle of the radii, a two-sided circuit (**FIG. 16**).

One of the modeling results is presented in **FIG. 17** where electric field strength above the resonator is shown. This shows the development of a spatial wave from the surface of the resonator (lower graph), side view. The graphs of the

distribution of the electric field strength in the figure were made for heights *z* above the surface of the resonator, from *z*=0, lower graph, to *z*=0.2 mm for the last, upper graph. The wave attenuates above a distance of 0.2 mm.

The figure **FIG. 18** also illustrates the strength by height in the same sections from different positions. Electric field strength on the surface of the resonator (lower graph, z= 0) and so on in layers above the surface: 0.1mm; 0.2mm; 0.3mm. When z>0.2mm, the wave decays.

Above the coordinate *z*=0.2 mm, the electric field strength becomes very small. The figure shows that it extends in breadth and the strength magnitude drops sharply with distance from the origin.

Impulse effect on two opposite points with grounded resonator center and two-sided circuit. The development of an electric field during rotation and given influence on two opposite points on both sides of the resonator was investigated. The figure **FIG. 19** presents the results of the calculation for the steady state, for a side view.

The figures **FIG. 20** from **FIG. 20a** to **FIG.20t** present the same result layer by layer for heights from 0 mm to 1.7 mm above the resonator's surface.

The figure **FIG. 21** presents the results of modeling using a three-dimensional non-stationary model (6), i.e., dynamics of changes in the strength of the field above the waffer. The upper left figure is time moment 1. The middle left figure is time moment 2. The lower left figure is time moment 3. The upper right figure is time moment 4. The middle right figure is time moment 5, and the lower right figure is time moment 6.

The change in the development of the wave along the z-axis, which is orthogonal to the wafer's surface, can be seen clearly in the figures **FIG. 22** and **FIG. 23**. The wafer is located on the left and occupies the position whose borders are denoted in the middle left figure by two bars. Given a wafer with a diameter of 6 mm, the wavelength along the z-axis is approximately 1.1 mm. The radiation incident upon the wafer was white noise. **FIG. 22** shows distribution of field strength E above the resonator from 0.28 to 14.18 (V/m) with incident radiation at 2.4 GHz. **FIG. 23** shows distribution of field intensity I over the resonator from 0.08 to 201.05 (W/m^2) with incident radiation at 2.4 GHz.

Thus, the self-affine surface topography transforms the radiation incident on it into a coherent form, even for a wide range of frequencies.

- It was shown in [1] that a coherent transformer, when excited by EM radiation, forms a stationary, multi-frequency coherent wave (hologram) in space, which is stable and soliton-like regardless of the boundary conditions [2]. Its shape does not change with changing boundary conditions. This means that the result of this transformation does not depend on the characteristics of the radiation incident on it.
- Our experiments have demonstrated that a semiconducting wafer with a self-affine topography on its surface transforms a broad spectrum of incident radiation into a coherent form. It redistributes the incident radiation in terms of its wavelength as well as its phase, in accordance with its topography. Its use opens up fundamentally new opportunities for creating a variety of devices:

  - coherent transformers that harmonize the interaction of several wave fronts;

  - broadband resonators with distribution of energy through a space that is self-similar and carries information about the amplitude, wavelength, and phase of incident radiation.
- This development will find application in the form of a protective device that transforms external radiation, including 5G communication systems (3.5-28 GHz), into a form that is harmonized with the inherent radiation of an organism's cells, thus making it safe for a biological object.

Based on the fact that biological objects are open physical systems that have an EM nature and function under conditions of constant exchange of energy and matter with the environment, they have a specific design for fixing the set of the molecular structural lattice's nodal centers, which are interconnected in a unified spatial matrix. Since the molecular structural lattice reflects a specific model of the fundamental interrelationships of the object, it is possible to consider the biological organization as an organization that initiates a constant EM superposition. This superposition is able to react by means of its own resonance to any particular

external impulse, causing changes in the molecular structure that gave rise to it, making it possible to have a targeted effect on the biological object.

As a result of the counter-harmonization of technogenic radiation interacting with the BO's own electromagnetic radiation, which is a superposition of cellular metabolism processes, the coherent transformer used in this method initiates optimization of the organism's adaptive physiological characteristics, thereby making the interaction conflict-free, which is proven by experimental data.

The essence of the claimed method is as follows.

The method for protecting biological objects from the negative influence of technogenic EM radiation in a wide range of frequencies, which includes creating around a biological object (BO) or between it and the source of technogenic EM radiation a special EM field in the form of a fractal coherent matrix (hologram), using a fractal-matrix coherent transformer to create the field.

The coherent transformer used is a self-affine lattice (resonator), formed from circular topological lines, creating a slit-like raster.

The resonator's structural lattice is a Fourier transformer that harmonizes the amplitudes, phases, frequencies and polarization vectors of external technogenic radiation and the BO's inherent EM radiation. The coherent field that forms around the resonator resonates with the surrounding EM waves, including with the inherent radiation of the human body's biological cells, transforming it into a consistent form, and makes the interaction conflict-free.

The resonator's coherently transforming impulse forms a spatial matrix whose multilevel gradation is a set of annular raster lattices symmetric with at least the three orthogonal basis vectors X, Y, Z with a subsequent release to multidimensionality N and with the formation of a spatial monostructural form with an infinite number of inherent components satisfying Noether's theorem, which requires the formation of the maximum spatial symmetry of the object's field structure, and the condition of interaction in the form of a self-affine hypersphere.

$$\sum_{k=1}^{n} X^k + \sum_{k=1}^{n} Y^k + \sum_{k=1}^{n} Z^k + \cdots + \sum_{k=1}^{n} N^k \to 0 \quad ,$$

where X, Y, Z, N are the fractalization vectors of the system of a annular self-affine circuit, k = 1..n is the number of circuit elements.

According to the Noether theorem, each continuous symmetry of a physical system corresponds to a certain law of conservation. In our case, the symmetry of the diffraction grating, formed from annular topological lines, unambiguously forms a coherent EM field, which is a hologram as a stable wave structure. This is confirmed by the principle of holograms (D. Gabor – Yu.N. Denisyuk), according to which any wave superposition carries the same properties as the regular structure that generated it.

During the proposed exposure to a coherently transformed EM field, the complex of the wave characteristics of the inherent radiation of the cells of a biological object is brought into a resonant state that is determined by strict fractal-matrix schematization, which causes the system to respond. Such counter-harmonization of the wave characteristics, by eliminating conflict, leads to the stabilization of all metabolic processes and, as a result, an increase in the BO's adaptive abilities under conditions of exposure to technogenic EM radiation [3, 4].

The wave characteristics and stabilization of the metabolic processes of the BO are harmonized by exposing it to an EM field coherently transformed by the resonator's self-affine annular grating. For the resonator's self-affine annular grating, we used the fractal-planar projection of a special spatial structural-holographic construction, fixed on a solid medium and formed from annular topological slit-like lines that create a raster (RF Patent No. 2231137, No. 2217181, No. 2284062).

The figures **FIG. 24a** and **FIG. 24b** show simplified versions of planar projections of the spatial structural-holographic self-affine matrix of the resonator's coherently transforming field response.

The coherently transforming resonator can be made in various embodiments, depending on its location, and be directly on the BO (attached to clothing, hung from a cord, etc.), near the biological object BO (for example, in the same room), attached to the source of technogenic EM radiation (mobile phone, computer, home appliances, etc.) or be between the BO and the radiation source.

The proposed method for protecting biological objects from technogenic EM radiation contributes to a reduction (elimination) of the negative influence of technogenic EM radiation on the BO, especially with the spread of 5G

communication systems. This method makes it possible to protect a biological object from the negative influence of broadband EM radiation.

The claimed method has no analogues and can be used in the daily life of a person that exists among a large number of electronic devices emitting an EM field.

CITATION LIST

Patent Literature

- Patent application WO1997034459A2, patent RU2194376. L. Eriksson. Method of producing a metallic layer on the surface of a detail for shielding against electromagnetic radiation.
- Patent RU2265898C2. Voronin I.V. et al. Method for manufacturing a screen for protection from electromagnetic emission.
- Patent application DE10039125A1 / Patent RU2234175C2. J.T.Kuehnert et al. Electromagnetic absorbing material and method for manufacturing this material and shielding devices.

Non Patent Literature

1. Kopyltsov A.V., Serov I.N., Lukyanov G.N. Interaction of a Semiconducting Wafer with a Self-Affine Surface Topography with Electromagnetic Radiation. Nanotechnology. - 2006. - No. 4(8). - pp. 44-49.
2. Serov I.N., Lukyanov G.N., Kopyltsov A.V. Mathematical Modeling of the Interaction of Electromagnetic Radiation with a Silicon Self-Affine Surface. ENGECON Bulletin, "Technical Sciences" series - 2007 Issue 6(19) - pp. 199-205.
3. Serov I.N., Sysoyev V.N., Rybina L.A., Ananeva V.N., Effect of products with a nano-scale fractal topology on several vital processes and human ecology, Nanotechnology, 2006, April, No. 1, pp. 146-151.
4. Serov I.N., V.N. Sysoyev., Evaluation of the effectiveness of using Aires Shield electromagnetic anomaly neutralizers to reduce the negative influence of the electromagnetic field caused by the operation of a cellular phone, International Journal of Applied and Fundamental Research. – 2014. – No. 8 – pp. 81-85.
5. Slabko V.V., Principles of Holography, Soros Educational Journal, No. 7, 1997.
6. D. Gabor."Holography (1948-1971)". Nobel Lecture, Advances in the Physical Sciences, Vol. 109, Issue 1, January 1973.

7. Yu. N. Denisyuk. Principles of Holography. — Leningrad: Publishing House of the State Optical Institute, 1979.

8. A.S. Mitrofanov. Principles of amplification of optical radiation. Teaching aid. Saint Petersburg. Saint Petersburg State University of Information Technologies, Mechanics, and Optics, 2005.

9. Potapov A.A., Fractals in Radiophysics and Radiolocation: Topology of the Sample. Edition 2, revised and added to. – Moscow: Universitetskaya Kniga, 2005.

10. Mandelbrot, V.V., *Self-affine fractals and fractal dimension,* Physica Scripta 32 (1985) 257–260.

11. Nguyen VD, Bouisset P, Kerlau G, Parmentier N, Akatov YA, Archangelsky VV, Smirenniy LN, Siegrist M. A new experimental approach in real time determination of the total quality factor in the stratosphere. *Rad. Prot. Dos.* 1993; 48(1): 41-46.

12. Johansen Ch. Electromagnetic fields and health effects - epidemiologic studies of cancer, diseases of the central nervous system and arrhythmia-related heart disease. *Scand J Work Environ Health* 2004; 30 Suppl 1: 1-80.

13. Hardell L, Sage C. Biological effects from electromagnetic field exposure and public exposure standards. *Biomedicine & Pharmacotherapy* 2008; 62: 104-109.

14. Terzia M, Ozberka B, Denizb OG, Kaplanb K. The role of electromagnetic fields in neurological disorders. *J. Chem. Neuroanatomy*. 2016; 75: 77-84.

15. Repacholi MH, Basten A, Gebski V, Noonan D, Finnie J, Harris, AW. Lymphomas in E mu-Pim1 transgenic mice exposed to pulsed 900 MHz electromagnetic fields. *Radiation Research*.1997; 147(5): 631-640.

16. Phillips JL, Singh NP, Lai H. Electromagnetic fields and DNA damage. *Pathophysiology* 2009; 16(2-3): 79-88.

CLAIMS

1. The method for protecting a biological object from the negative influence of technogenic electromagnetic radiation in a wide range of frequencies, c h a r a c t e r i z e d in that it includes creating around the biological object or between the biological object and the source of technogenic electromagnetic radiation a special electromagnetic field in the form of a fractal coherent matrix.

2. The protection method according to claim 1, c h a r a c t e r i z e d in that the field is created using a fractal-matrix coherent transformer which is a self-affine lattice of annular topological lines creating a slit-like raster.

3. The protection method according to claim 1, c h a r a c t e r i z e d in that the coherent transformer forms an electromagnetic field in the form of a spatial holographic matrix.

4. The protection method according to claim 1, c h a r a c t e r i z e d in that the transformer's electromagnetic field transforms the technogenic electromagnetic radiation into the form of a spatial coherent matrix of harmonized electromagnetic wave superpositions.

5. The protection method according to claim 1, c h a r a c t e r i z e d in that depending on the nature of the negative influence, different options for placement of the coherent transformer are used: on a biological object.

6. The protection method according to claim 1, c h a r a c t e r i z e d in that depending on the nature of the negative influence, different options for placement of the coherent transformer are used: on a source of technogenic electromagnetic radiation.

7. The protection method according to claim 1, c h a r a c t e r i z e d in that depending on the nature of the negative influence, different options for placement of the coherent transformer are used: between a biological object and a source of technogenic electromagnetic radiation.

AMENDED CLAIMS
received by the International Bureau on 01 October 2020 (01.10.2020)

1. The method for transforming an electromagnetic radiation in a range of frequencies, characterized in that said electromagnetic radiation is transformed into the coherent electromagnetic radiation.

2. The method according to claim 1, characterized in that the electromagnetic radiation is transformed using a fractal-matrix coherent transformer, which is an electromagnetic field formed by a self-affine lattice of annular topological lines creating a slit-like raster.

3. The method according to claim 1, characterized in that the coherent transformer is an electromagnetic field in the form of a regular spatial holographic matrix.

4. The method according to claim 1, characterized in that the transformer's electromagnetic field transforms the electromagnetic radiation into the form of a spatial coherent matrix of harmonized electromagnetic wave superpositions.

5. The method according to claim 1, characterized in that the placement of the coherent transformer, providing said formed electromagnetic field, is used: on a biological object.

6. The method according to claim 1, characterized in that the placement of the coherent transformer, providing said formed electromagnetic field, is used: on a source of the electromagnetic radiation.

7. The method according to claim 1, characterized in that the placement of the coherent transformer, providing said formed electromagnetic field, is used: between a biological object and a source of the electromagnetic radiation.

8. The method according to claim 1, characterized in that the range of frequencies of the electromagnetic radiation is from 2,4 Ghz to 28 Ghz.

9. The method according to claim 1, characterized in that the electromagnetic radiation to be transformed into the coherent form is a technogenic electromagnetic radiation emitted by any technical devices and systems.

Statement under Article 19(1)

In view of the PCT INTERNATIONAL SEARCH REPORT Office Action, amendments for the CLAIMS are being proposed.

The independent Claim 1 now defines a method of transforming the electromagnetic radiation (electromagnetic field) in a range of frequences into a coherent electromagnetic radiation. The observed deficiences and unclear terms were removed from claims in order Claim 1 to describe the method as a technical solution to transform an electromagnetic radiation (electromagentic field) in a range of frequencies into its coherent form of the frequency-amplitude spectrum.

The claims 2 to 7 were amended to remove unclear and non-technical terms that have been identified in the International Search Report.

A new Claim 8 has been added, in order to define the range of frequences 2.4-28GHz of the electromagnetic radiation to be transformed.

A new Claim 9 has been added, in order to define a particular type of electromagnetic radiation to be transformed which is emitted by technical systems and devices, otherwise known as technogenic electromagnetic radiation.

DRAWINGS

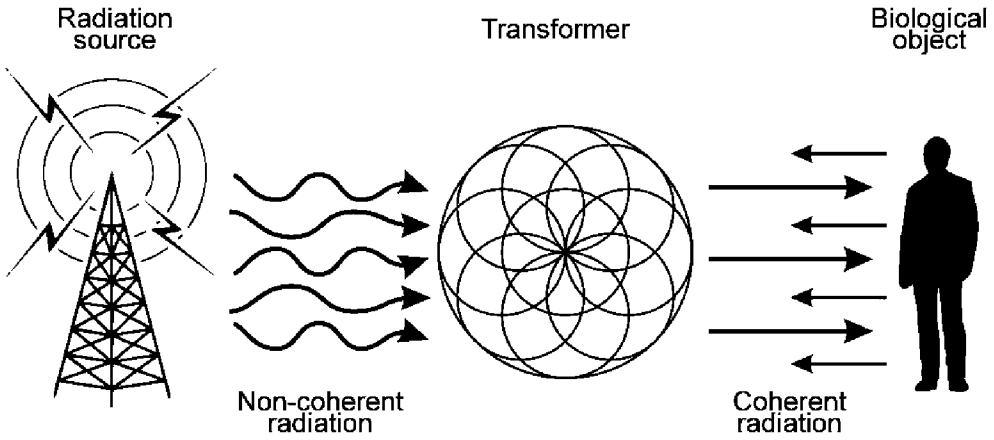

FIG. 1

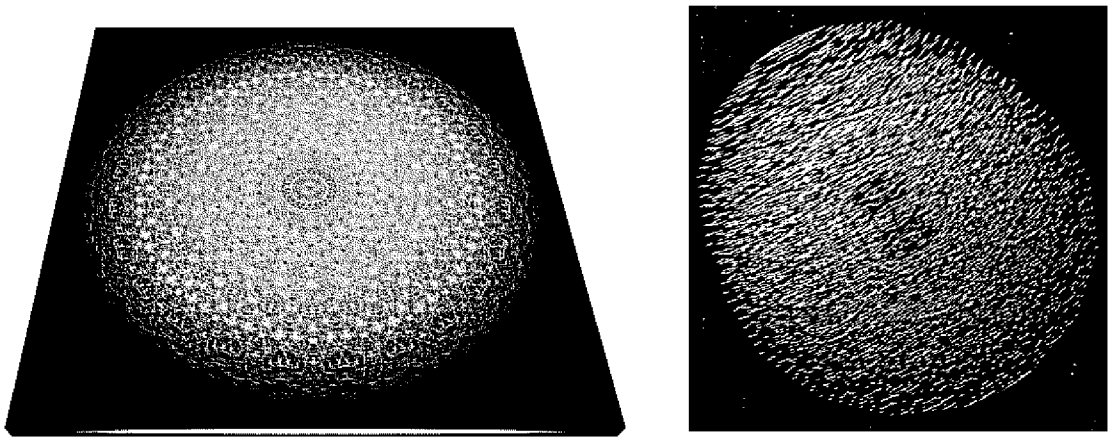

(a) (b)

FIG. 2

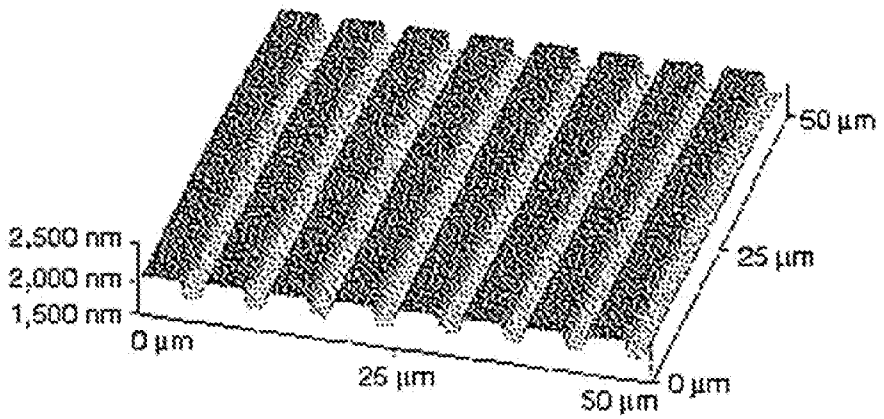

FIG. 3

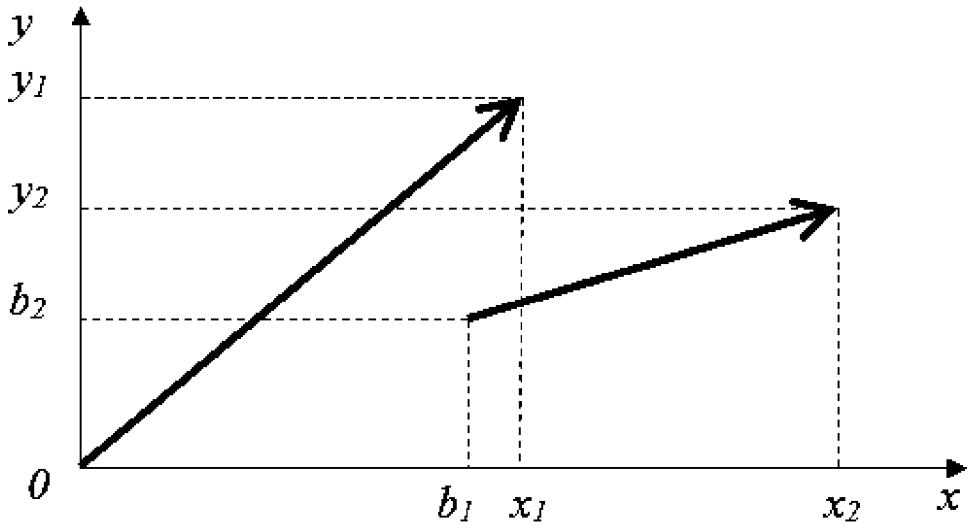

FIG. 4

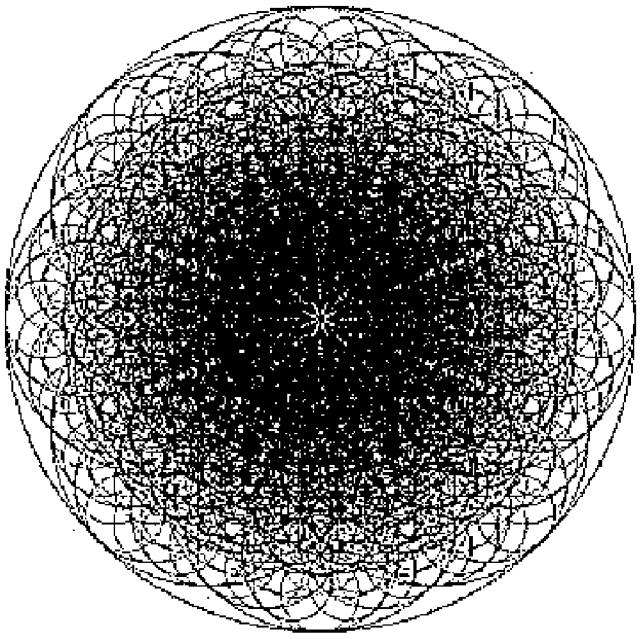

Result of performing affine transformations

FIG. 5

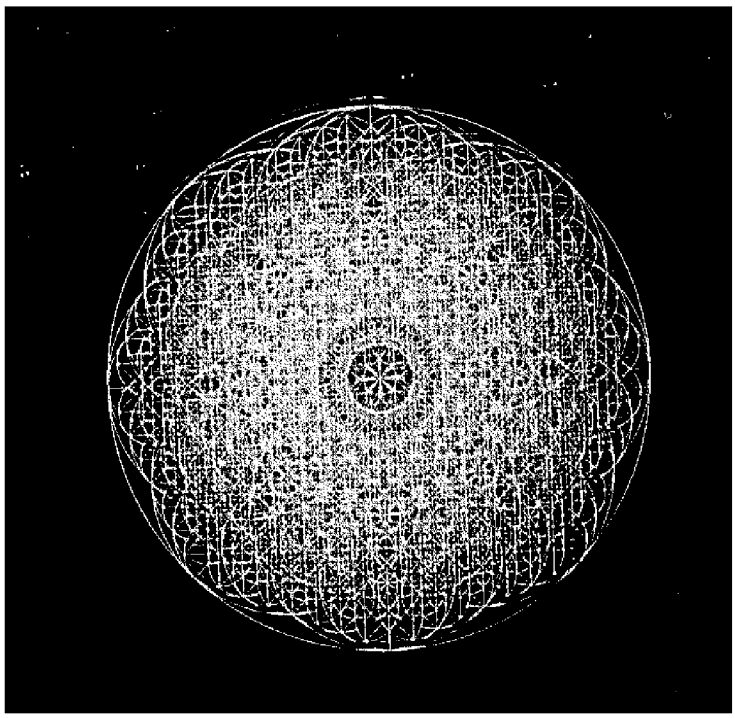

FIG. 6

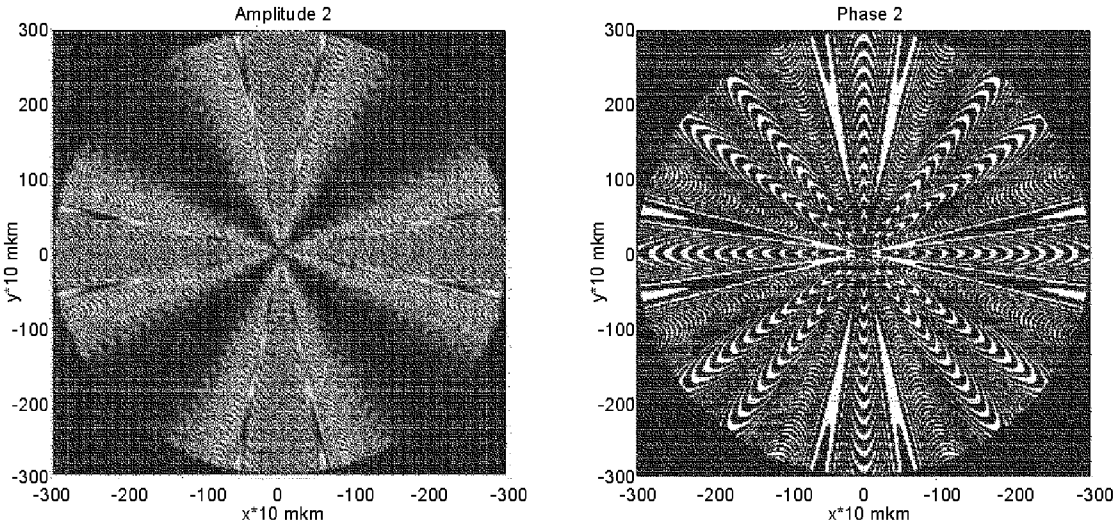

(a) (b)

FIG. 7

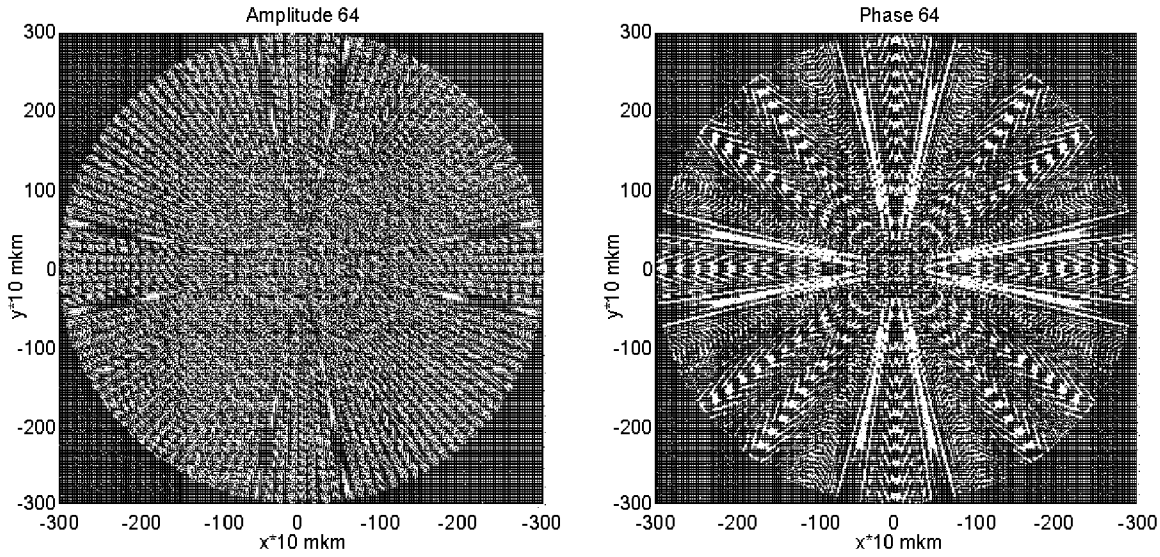

(a) (b)

FIG. 8

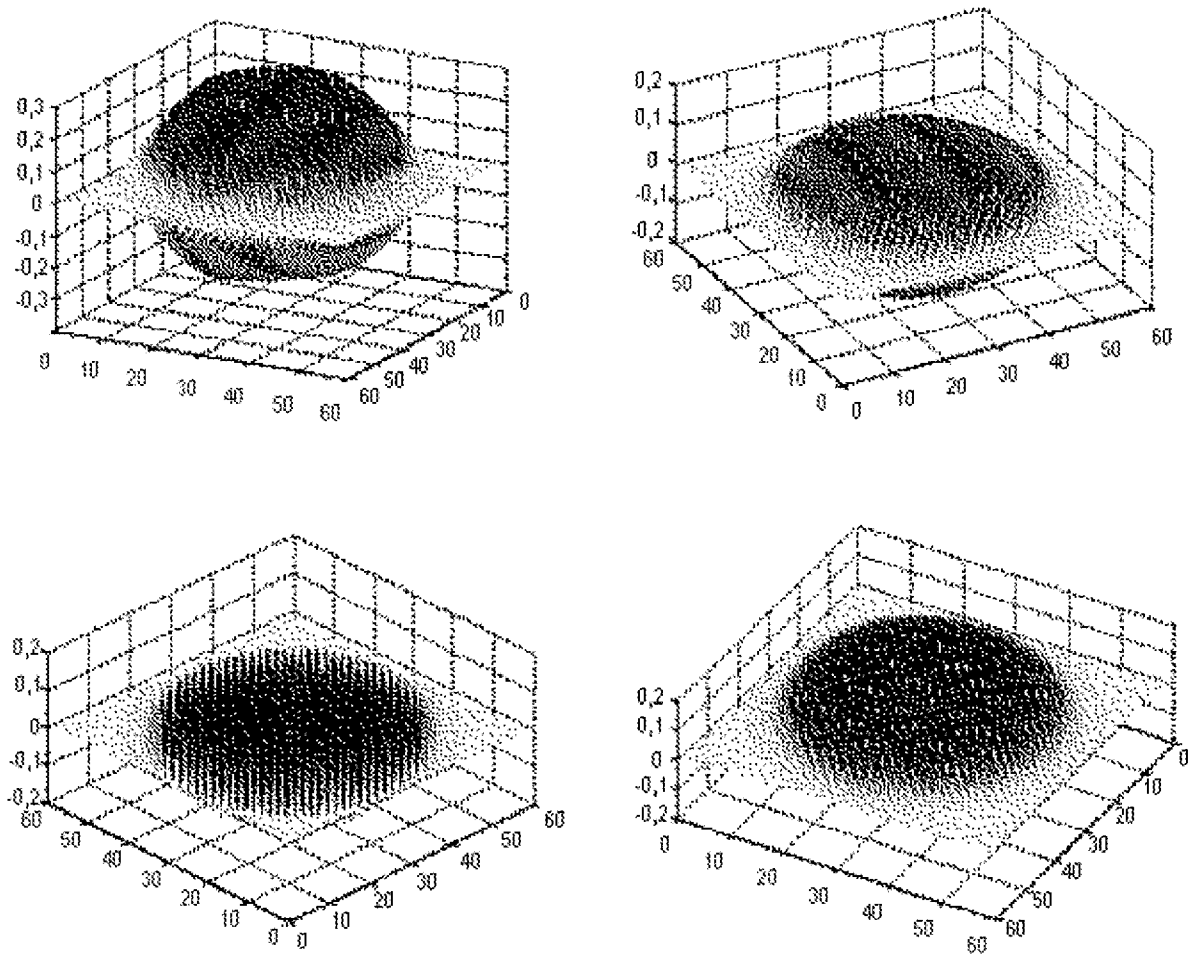

FIG. 9

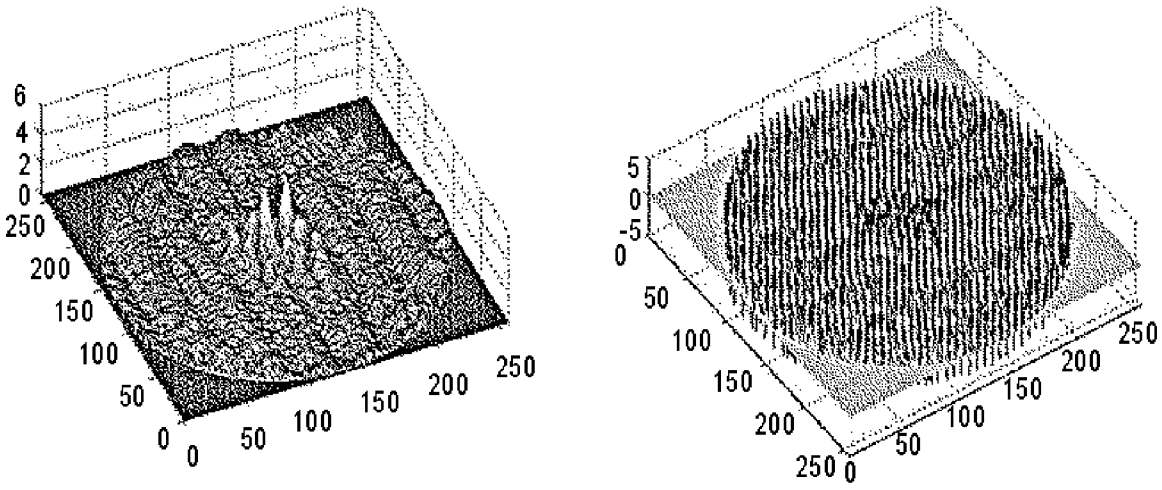

(a) (b)

FIG. 10

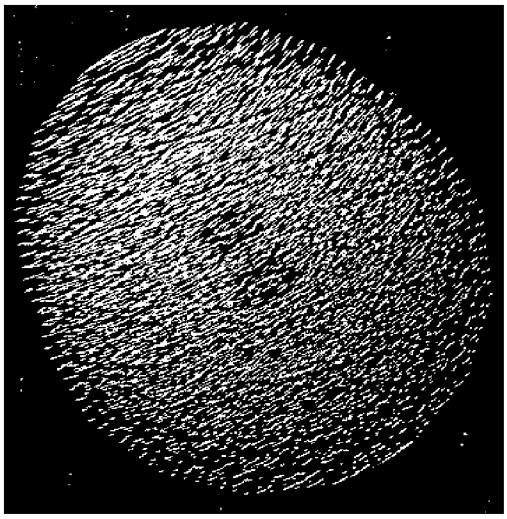

FIG. 11

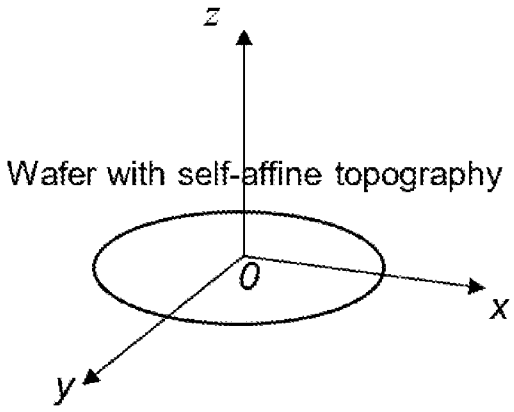

Wafer orientation relative to the coordinate system

FIG. 12

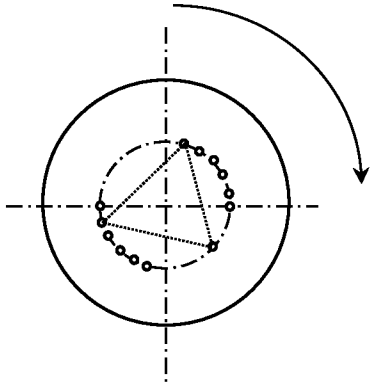

FIG. 13

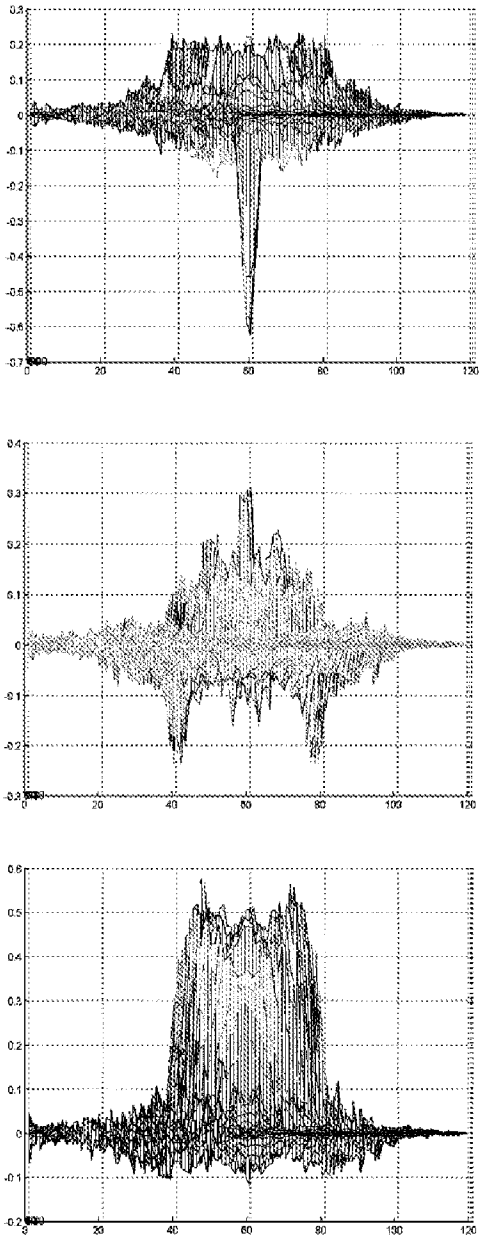

FIG. 14

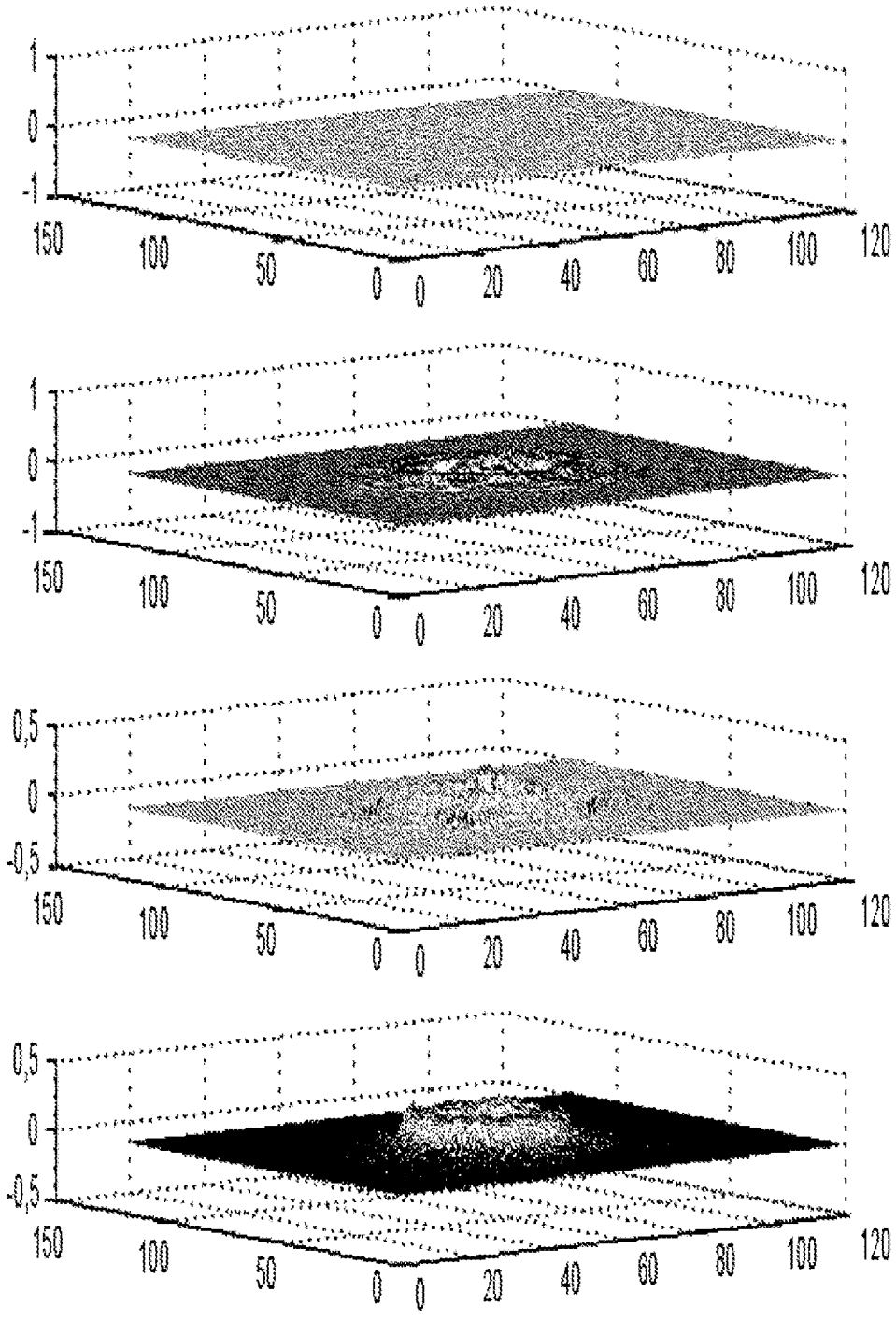
1
0
-1
150
100
50
0
0
20
40
60
80
100
120
1
0
-1
150
100
50
0
0
20
40
60
80
100
120
0,5
0
-0,5
150
100
50
0
0
20
40
60
80
100
120
0,5
0
-0,5
150
100
50
0
0
20
40
60
80
100
120

FIG. 15

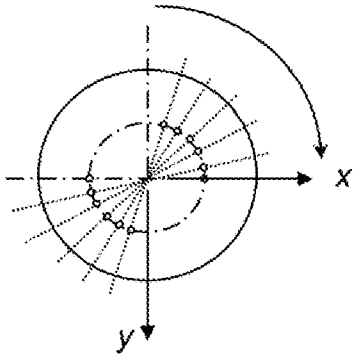

FIG. 16

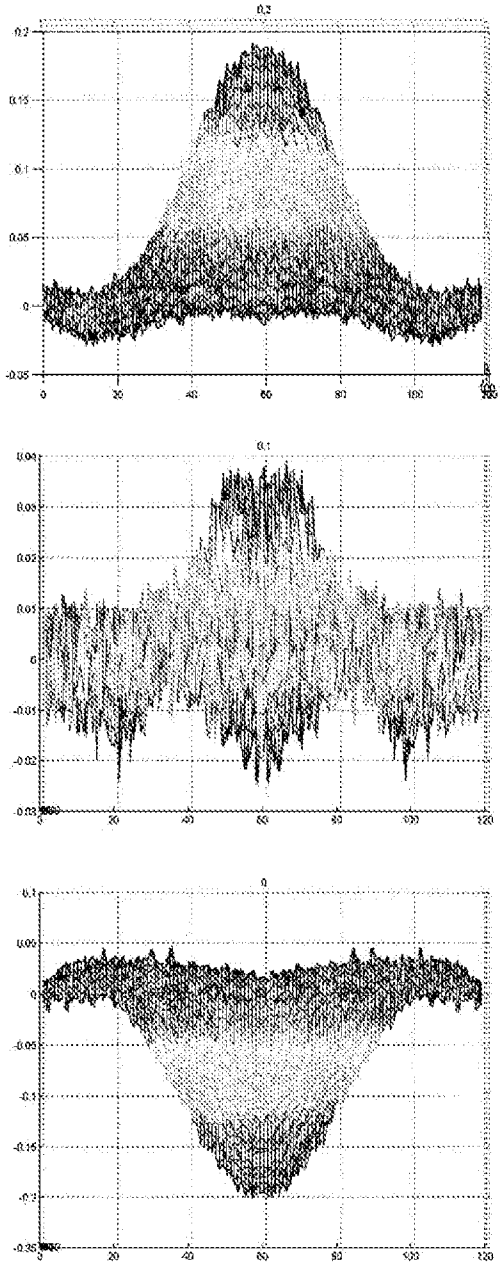

FIG. 17

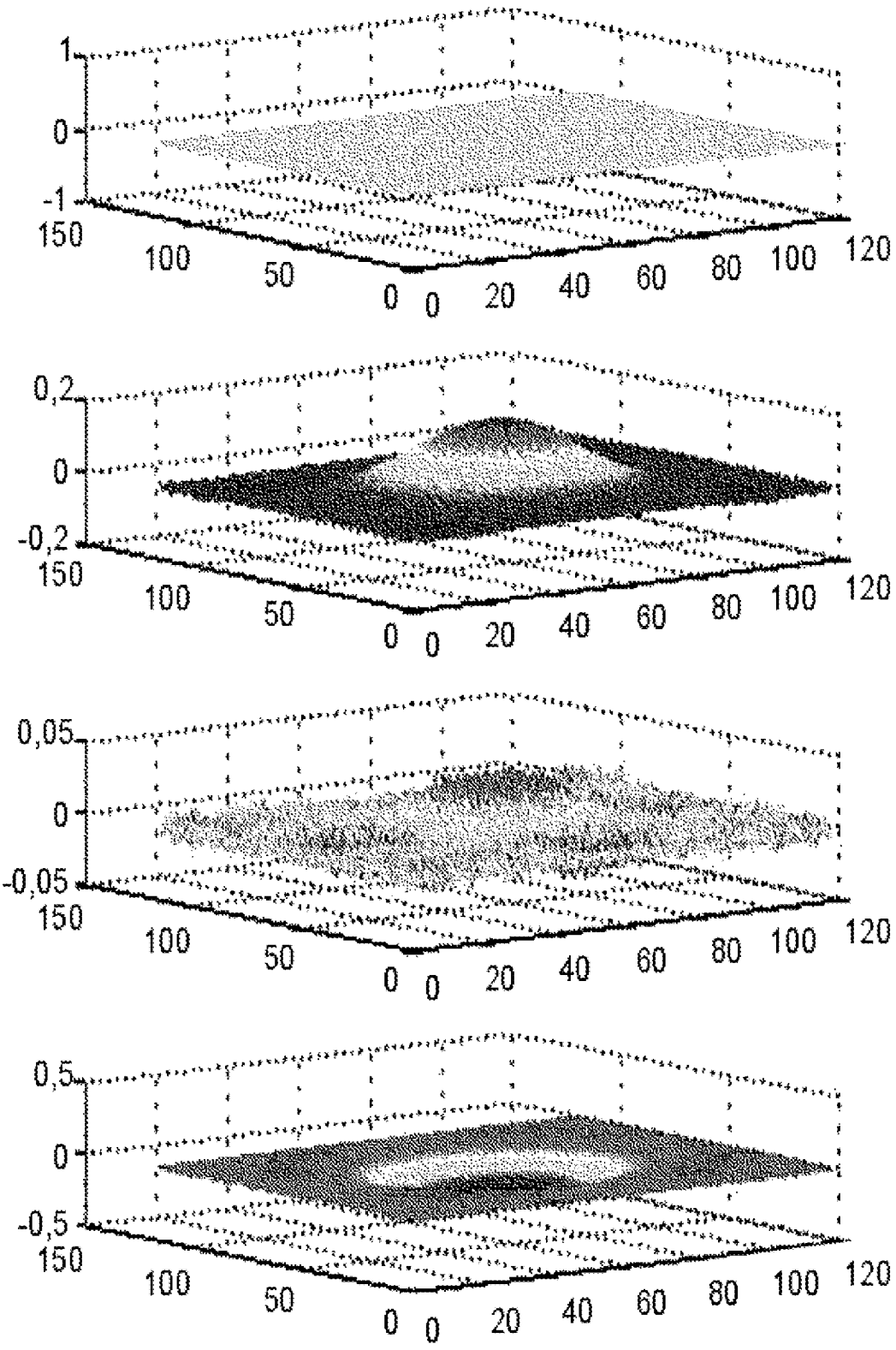

FIG. 18

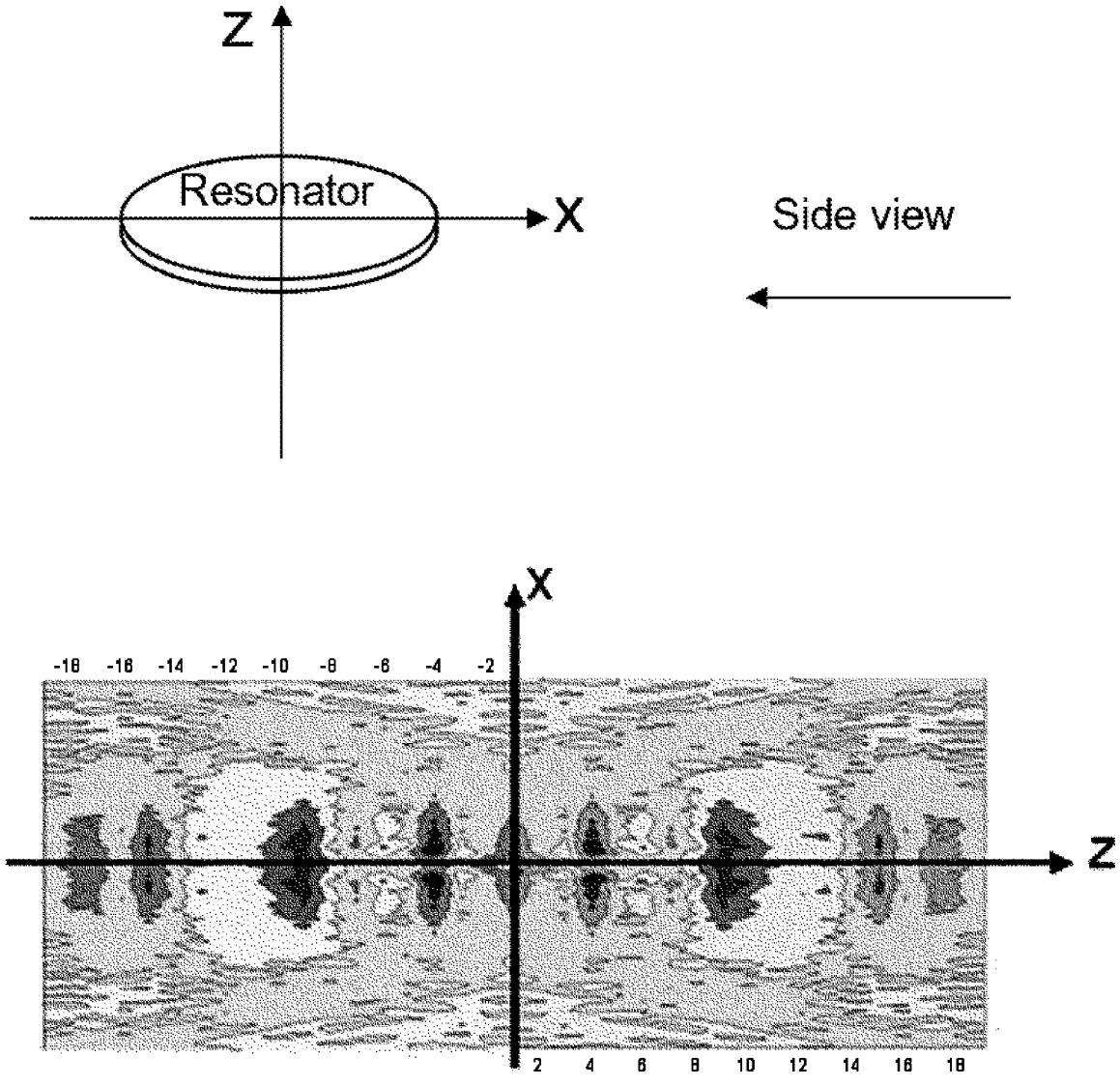

FIG. 19

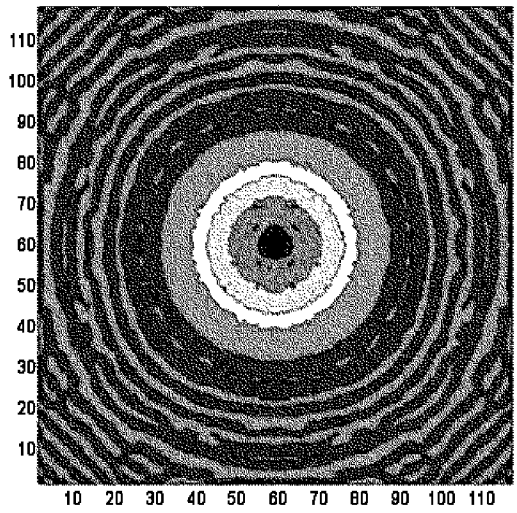

(a) on surface

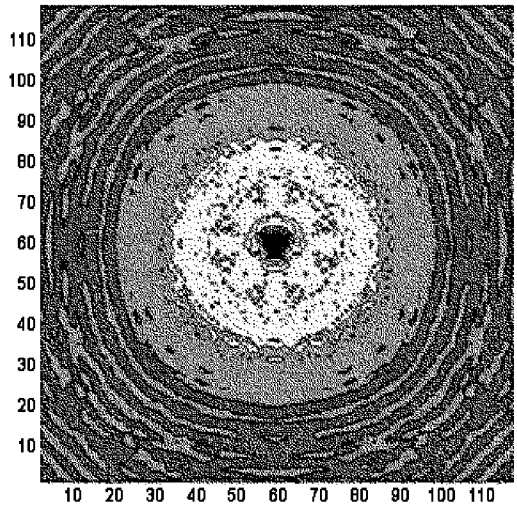

(b) at 0.1 mm

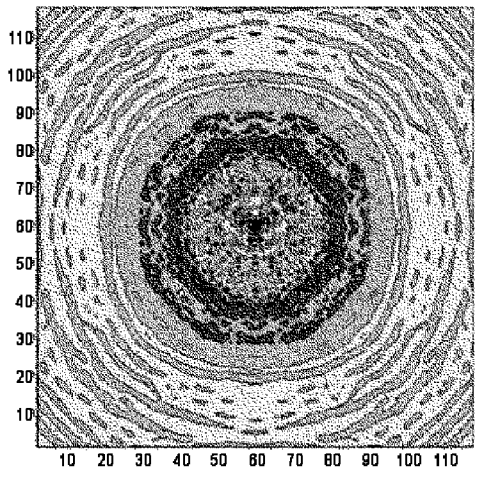

(c) at 0.2 mm

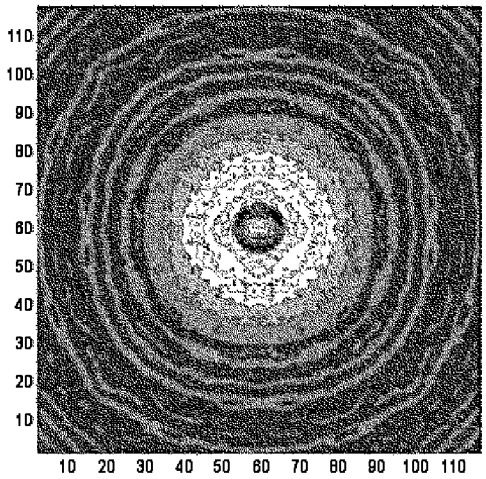

(d) at 0.3 mm

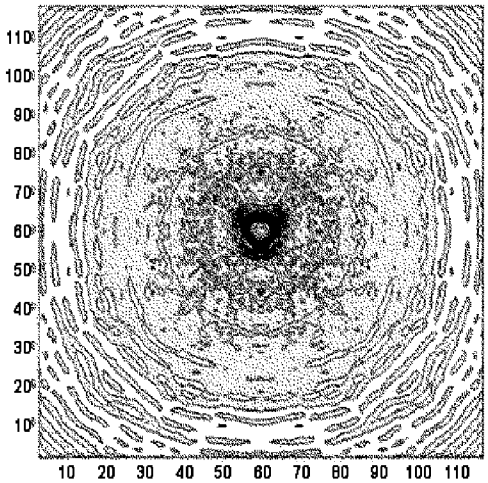

(e) at 0.4 mm

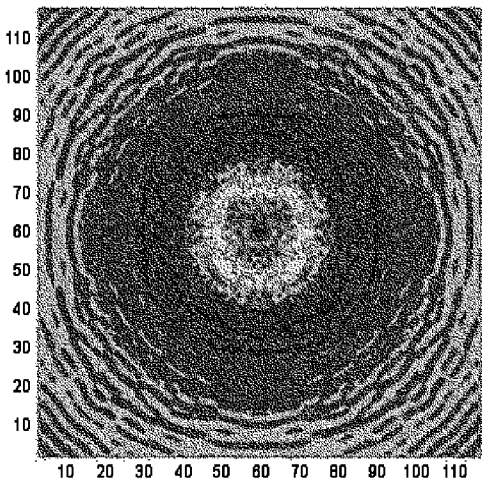

(f) at 0.5 mm

FIG. 20

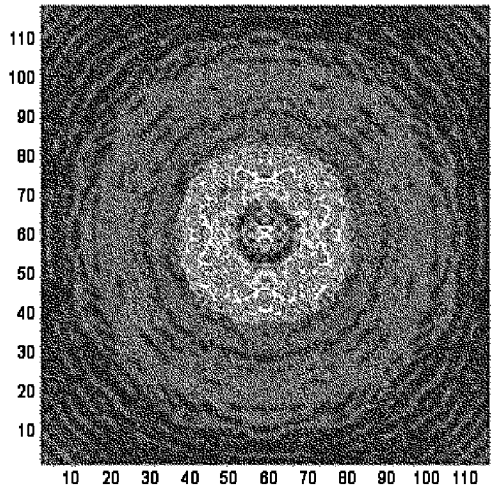

(g) at 0.6 mm

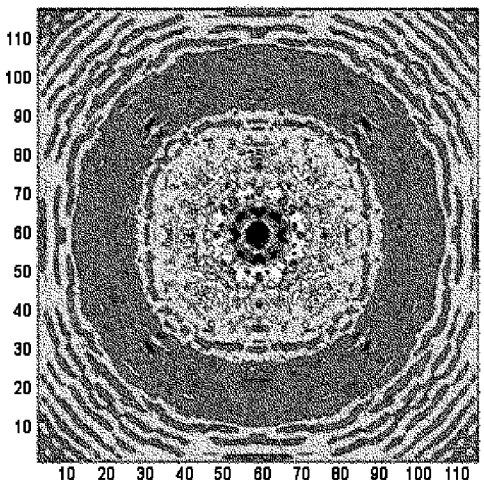

(h) at 0.7 mm

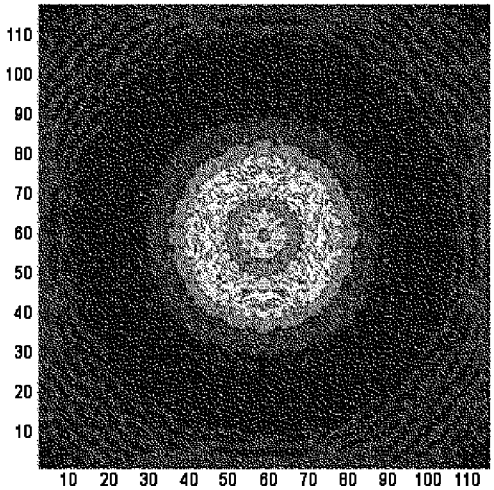

(i) at 0.8 mm

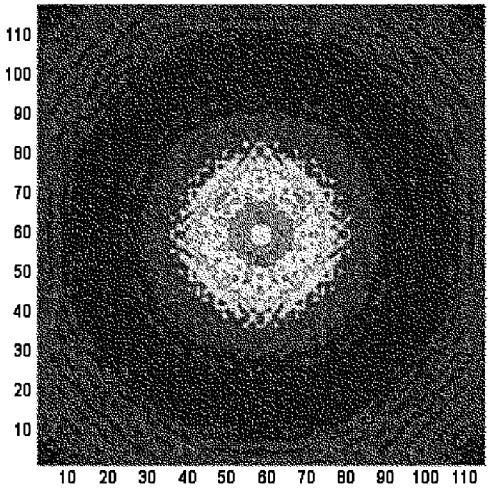

(k) at 0.9 mm

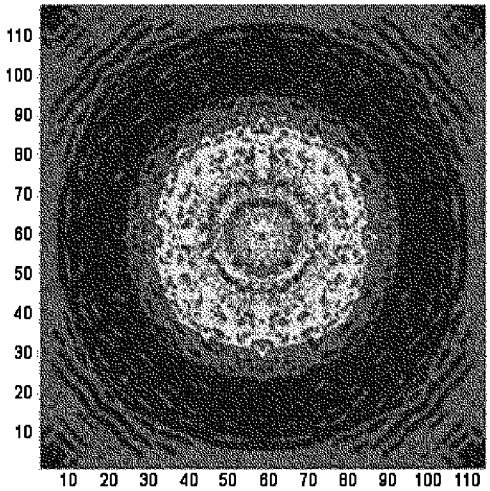

(l) at 1.0 mm

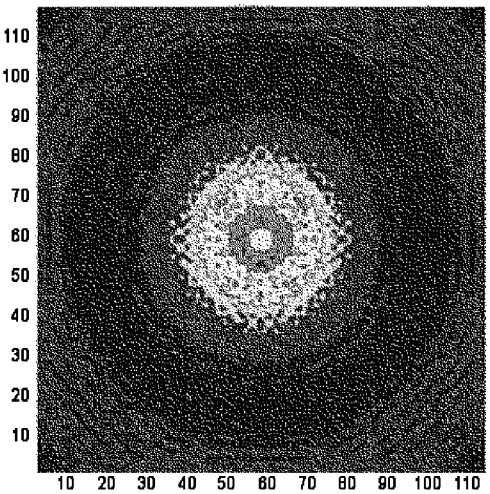

(m) at 1.1 mm

FIG. 20

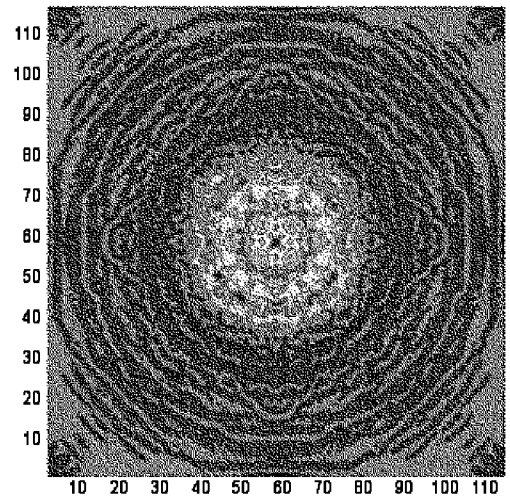

(n) at 1.2 mm

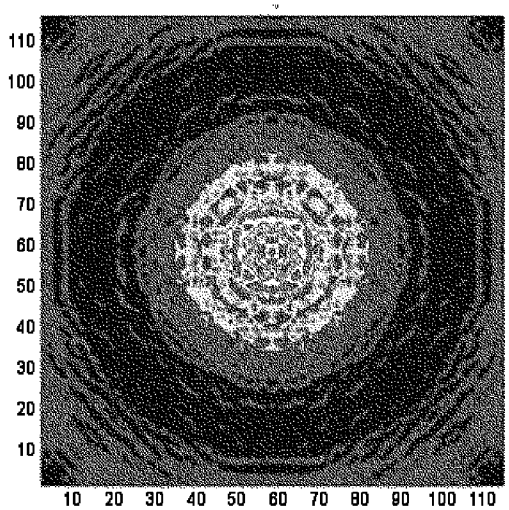

(o) at 1.3 mm

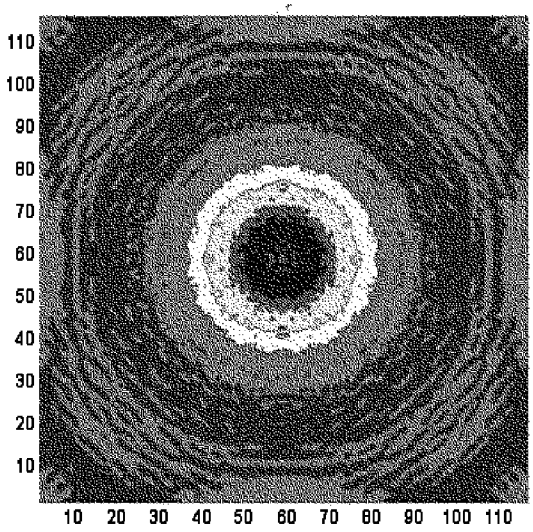

(p) at 1.4 mm

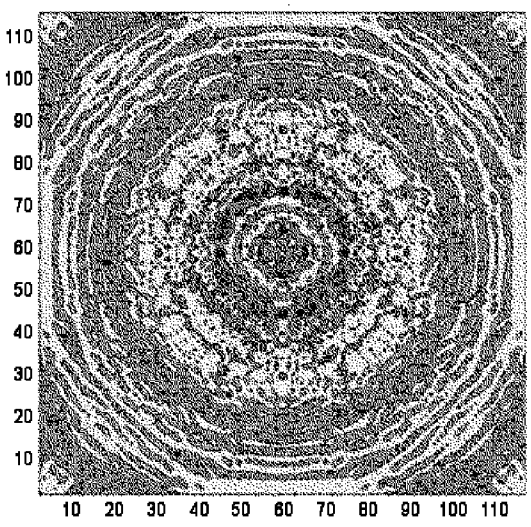

(r) at 1.5 mm

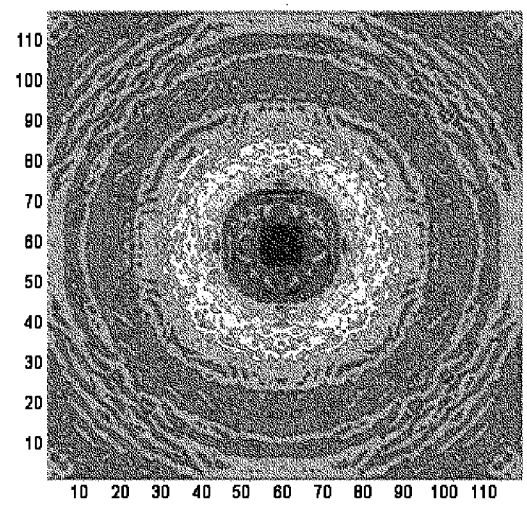

(s) at 1.6 mm

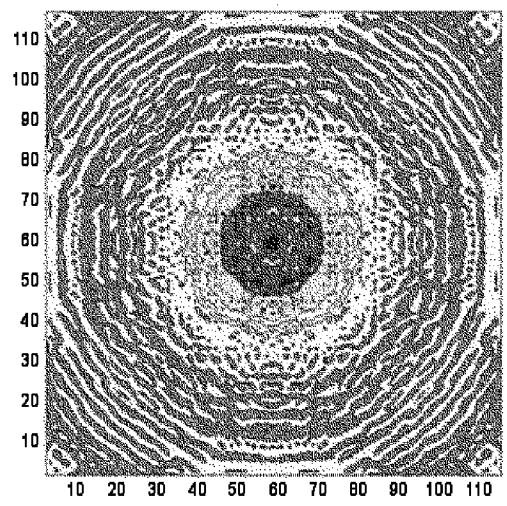

(t) at 1.7 mm

FIG. 20

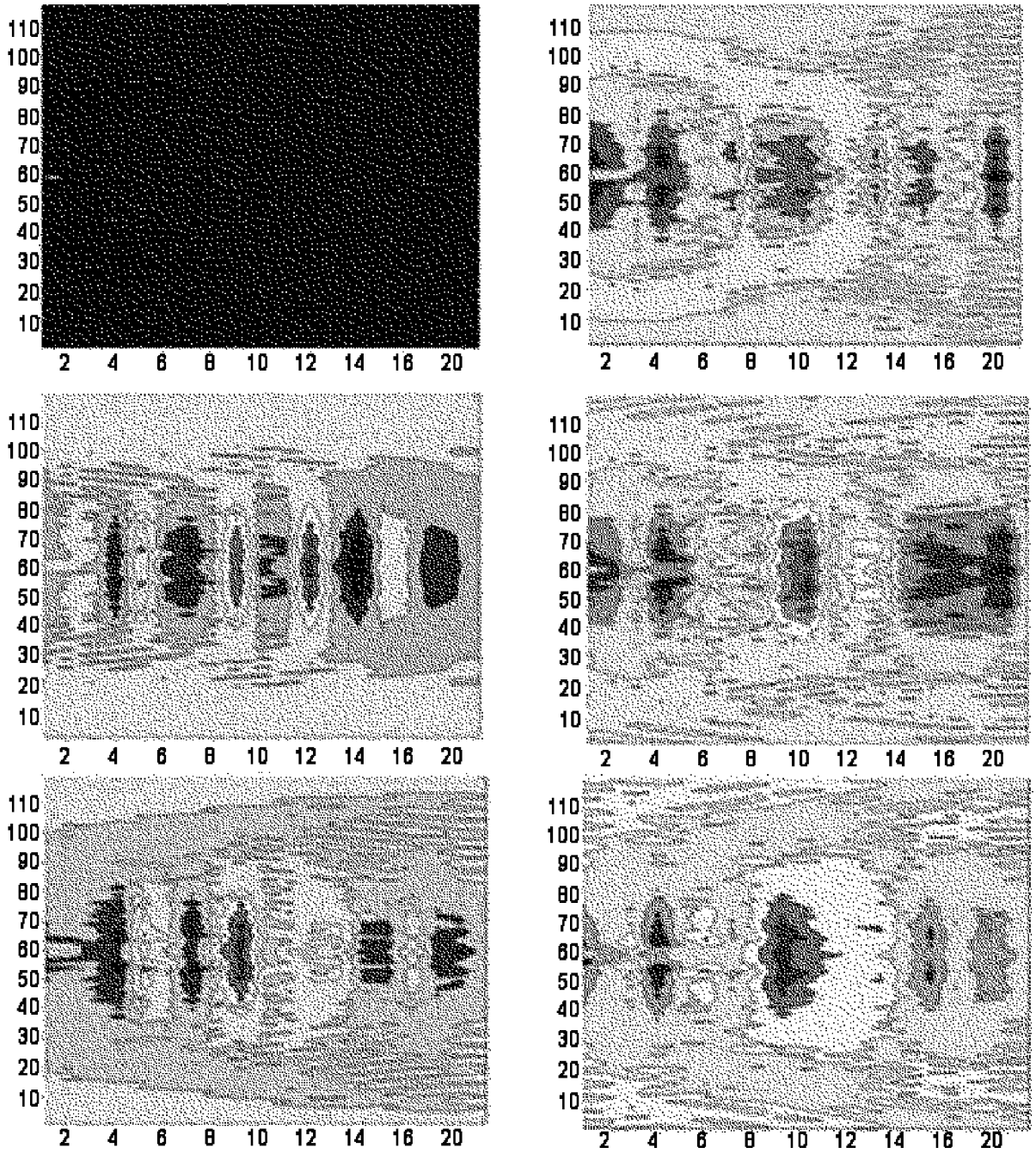

FIG. 21

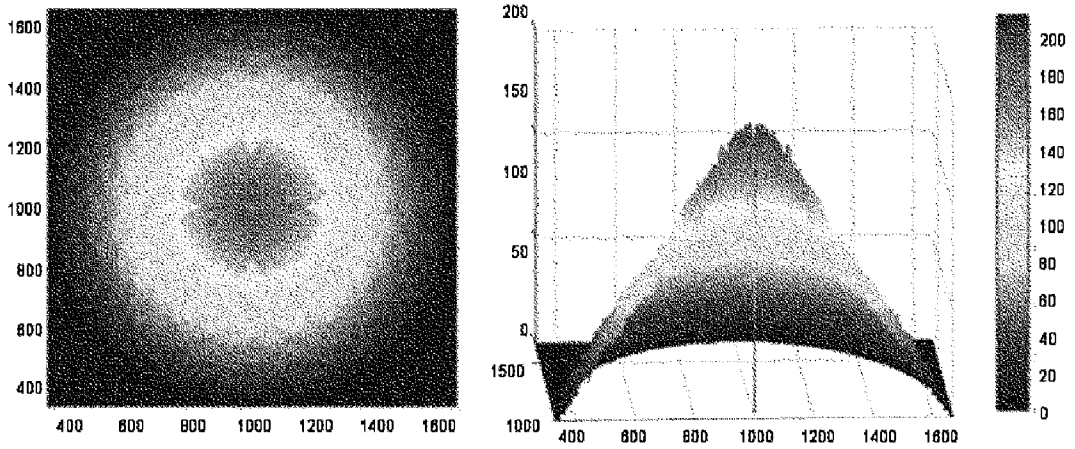

FIG. 22

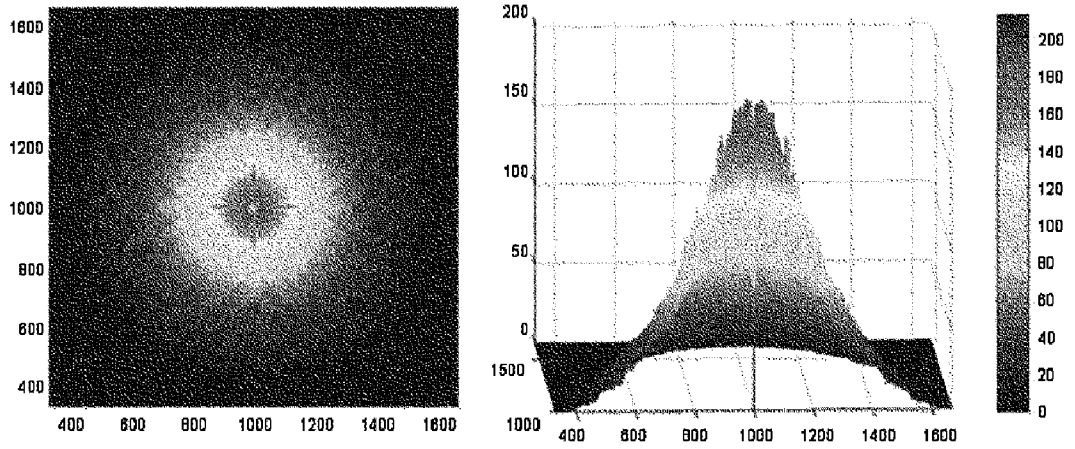

FIG. 23

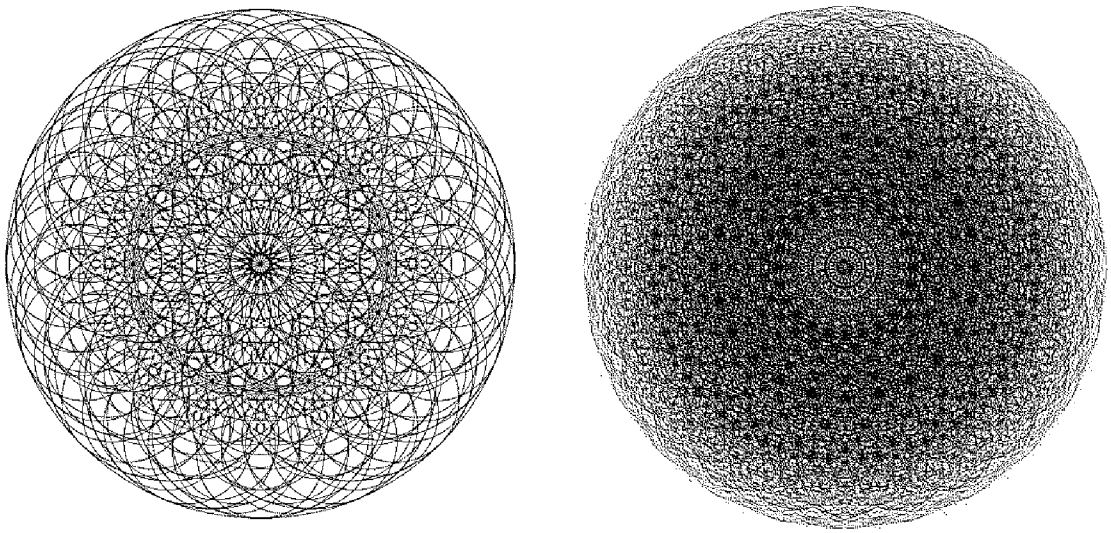

(a) (b)

FIG. 24

INTERNATIONAL SEARCH REPORT

International application No
PCT/IB2019/058334

A. CLASSIFICATION OF SUBJECT MATTER
INV. A61N1/16
ADD.

According to International Patent Classification (IPC) or to both national classification and IPC

B. FIELDS SEARCHED

Minimum documentation searched (classification system followed by classification symbols)
A61N

Documentation searched other than minimum documentation to the extent that such documents are included in the fields searched

Electronic data base consulted during the international search (name of data base and, where practicable, search terms used)
EPO-Internal, WPI Data

C. DOCUMENTS CONSIDERED TO BE RELEVANT

Category*	Citation of document, with indication, where appropriate, of the relevant passages	Relevant to claim No.
X	RU 2 231 137 C1 (SEROV, IGOR) 20 June 2004 (2004-06-20) cited in the application paragraphs [0036], [0043]	1-7
X	RU 2 308 065 C1 (SEROV IGOR NIKOLAEVICH [RU]) 10 October 2007 (2007-10-10) paragraphs [0001], [0007], [0008], [0029]; claim 1	1-7
X	RU 2 200 968 C2 (SEROV IGOR NIKOLAEVICH) 20 March 2003 (2003-03-20) paragraphs [0015], [0016]	1-7
X	US 2011/065975 A1 (KAZANSKIY LEONID [HK]) 17 March 2011 (2011-03-17) paragraphs [0019] - [0021]	1-7

-/--

[X] Further documents are listed in the continuation of Box C.

[X] See patent family annex.

* Special categories of cited documents :

"A" document defining the general state of the art which is not considered to be of particular relevance

"E" earlier application or patent but published on or after the international filing date

"L" document which may throw doubts on priority claim(s) or which is cited to establish the publication date of another citation or other special reason (as specified)

"O" document referring to an oral disclosure, use, exhibition or other means

"P" document published prior to the international filing date but later than the priority date claimed

"T" later document published after the international filing date or priority date and not in conflict with the application but cited to understand the principle or theory underlying the invention

"X" document of particular relevance; the claimed invention cannot be considered novel or cannot be considered to involve an inventive step when the document is taken alone

"Y" document of particular relevance; the claimed invention cannot be considered to involve an inventive step when the document is combined with one or more other such documents, such combination being obvious to a person skilled in the art

"&" document member of the same patent family

Date of the actual completion of the international search	Date of mailing of the international search report
9 June 2020	22/06/2020

Name and mailing address of the ISA/	Authorized officer
European Patent Office, P.B. 5818 Patentlaan 2 NL - 2280 HV Rijswijk Tel. (+31-70) 340-2040, Fax: (+31-70) 340-3016	Büchler Costa, Joana

INTERNATIONAL SEARCH REPORT

International application No
PCT/IB2019/058334

C(Continuation). DOCUMENTS CONSIDERED TO BE RELEVANT

Category*	Citation of document, with indication, where appropriate, of the relevant passages	Relevant to claim No.
A	US 2016/001091 A1 (HASSLER RICHARD MICHAEL [US] ET AL) 7 January 2016 (2016-01-07) paragraphs [0031], [0032]	1-7

INTERNATIONAL SEARCH REPORT

Information on patent family members

International application No
PCT/IB2019/058334

Patent document cited in search report	Publication date	Patent family member(s)	Publication date
RU 2231137 C1	20-06-2004	NONE	
RU 2308065 C1	10-10-2007	NONE	
RU 2200968 C2	20-03-2003	NONE	
US 2011065975 A1	17-03-2011	LT 5768 B	26-09-2011
		US 2011065975 A1	17-03-2011
US 2016001091 A1	07-01-2016	US 2016001091 A1	07-01-2016
		US 2018126118 A1	10-05-2018